






# Integration of Mid-Infrared Light Sources on Silicon-Based Waveguide Platforms in 3.5–4.7 $\mu\text{m}$ Wavelength Range

Aditya Malik , Alexander Spott , Graduate Student Member, IEEE, Eric J. Stanton, Jonathan D. Peters, Jeremy Daniel Kirch, Luke J. Mawst , Fellow, IEEE, Dan Botez , Life Fellow, IEEE, Jerry R. Meyer, Fellow, IEEE, and John E. Bowers , Fellow, IEEE

(Invited Paper)

**Abstract**—Mid-infrared light sources are attracting attention for use in spectroscopic sensing, thermal imaging, and infrared countermeasures. Integration of these sources on Si-based waveguides allows for more functional and complex photonic circuits to be integrated on a single chip. This paper focuses on the key aspects of this integrated platform. The operation of silicon-on-insulator waveguides beyond 4.0  $\mu\text{m}$  wavelength with increasing waveguide core thickness is discussed, and the effects of various cladding materials on waveguide propagation loss is demonstrated. Low loss waveguides and Mach-Zehnder interferometers in Ge-on-Si waveguide platform are discussed and beam combiners in the form of arrayed waveguide gratings are demonstrated in both the platforms. Interband cascade lasers are integrated on silicon-on-insulator waveguides with direct bonding to realize Fabry-Perot lasers. Power scaling of integrated lasers is validated by integrating quantum cascade lasers with silicon-on-insulator beam combiners. Results for the first integrated Fabry-Perot quantum cascade lasers on Ge-on-Si waveguides are discussed, together with the potential use of these waveguides to provide a better heat sink for integrated mid-infrared light sources.

**Index Terms**—Semiconductor waveguides, silicon photonics, quantum cascade lasers, interband cascade lasers.

Manuscript received February 20, 2019; revised October 17, 2019; accepted October 17, 2019. Date of publication October 24, 2019; date of current version November 22, 2019. This material is based on research sponsored in part by Air Force Research Laboratory under agreement number FA8650-15-2-5220 and in part by the Office of Naval Research under Grant N00014-13-C-0147. (Corresponding author: Aditya Malik.)

A. Malik, A. Spott, J. D. Peters, and J. E. Bowers are with the Department of Electrical and Computer Engineering, University of California Santa Barbara, Santa Barbara, CA 93106 USA (e-mail: amalik@ece.ucsb.edu; spott@ece.ucsb.edu; peters@ece.ucsb.edu; bowers@ece.ucsb.edu).

E. J. Stanton was with the Department of Electrical and Computer Engineering, University of California, Santa Barbara, Santa Barbara, CA 93106 USA. He is now with Applied Physics Division, National Institute of Standards and Technology, Boulder, CO 80305 USA (e-mail: eric.stanton@nist.gov).

J. D. Kirch, L. J. Mawst, and D. Botez are with the Department of Electrical and Computer Engineering, University of Wisconsin, Madison, WI 53706 USA (e-mail: jdkirch@wisc.edu; mawst@engr.wisc.edu; botez@engr.wisc.edu).

J. R. Meyer is with the Naval Research Laboratory, Washington, DC 20375 USA (e-mail: jerry.meyer@nrl.navy.mil).

Color versions of one or more of the figures in this article are available online at <http://ieeexplore.ieee.org>.

Digital Object Identifier 10.1109/JSTQE.2019.2949453

## I. INTRODUCTION

INTEGRATION of light sources on silicon based waveguide platforms provides a step closer towards realization of cheap, hand-held and robust optical systems. Silicon based waveguides are today fabricated in state-of-the-art CMOS pilot lines on substrates as large as 300 mm which lowers the cost of a single element substantially [1]. Heterogeneous integration of light producing compounds with silicon based photonic integrated circuits (PICs) allows optimized materials to be chosen for each desired function such as for gain, modulation, or detection. As compared to other integration approaches [2], heterogeneous integration approach doesn't require any active alignment between the integrated elements, which can be processed with the same high precision deep ultra violet (DUV) lithography tools as used for silicon processing. There are two versions of the heterogeneous integration approach the first being where two wafers or chips are bonded directly after plasma activation while the second requires an intermediate adhesive layer in between [3]. While both approaches use the same principles for transferring light between the laser diode and passive silicon-based waveguide, the first approach allows for better heat sink while the second lowers the tolerance of surface quality of both wafers. A significant amount of research has substantially advanced the heterogeneous integration of telecom and datacom wavelength range light emitting diodes on silicon-on-insulator (SOI) waveguides [4]–[6]. The SOI waveguides are typically made with a silicon device layer thickness between 220 nm–500 nm and with a buried oxide (BOX) layer of thickness between 1–2  $\mu\text{m}$ . The amount of functionality and complexity that can be introduced by using heterogeneous integration of light sources with such SOI based PICs has been demonstrated by realizing over 300 active components operating at 2.5 Tbps/cm bandwidth density on a single die [7].

However, applications such as chemical/biological sensing, thermal imaging, and infrared countermeasures require optical sources emitting at wavelengths beyond the telecom window. In particular, many atmospheric gases and biological fluids exhibit distinct and much stronger optical absorption features in the mid-infrared and longwave infrared spectral bands. High

power, single frequency light sources for these applications can be provided by III-V semiconductor based epitaxial materials. InP-based type I and type II laser diodes can emit light up to  $2.6 \mu\text{m}$ , while the operation wavelength can be pushed a little beyond  $3 \mu\text{m}$  using conventional type-I GaSb-based diode lasers. When these types of light sources have been integrated on standard SOI waveguides, the performance has been similar to their telecom counterparts [8]–[10].

While historically it has been much more challenging to develop semiconductor lasers that maintain high performance at wavelengths beyond  $3 \mu\text{m}$ , it is now known to be highly beneficial when multiple gain stages are stacked in a cascaded staircase. For wavelengths between  $3$  and  $6 \mu\text{m}$ , the interband cascade laser (ICL) [11], which employs type-II active quantum wells grown on a GaSb substrate, operates at threshold current and power densities only a little higher than those of optimized conventional diodes emitting in the near infrared. Furthermore, at wavelengths longer than  $\approx 4 \mu\text{m}$  (and extending to the THz regime), the quantum cascade laser (QCL) [12] can emit higher power than an ICL, although at the expense of a higher drive power to reach threshold. The InP-based QCL is unique in its use of optical transitions between two conduction subbands, rather than the electron-hole processes employed by all other semiconductor lasers. We previously demonstrated the heterogeneous integration of QCLs on silicon-on-nitride-on-oxide (SONOI) platforms, culminating in demonstrations of Fabry-Perot (FP) [13] and distributed feedback (DFB) QCLs operating at  $4.7 \mu\text{m}$  [14]. In addition to wafer bonding, direct growth of QCLs on a silicon substrate has also been reported [15]. Another approach of coupling light from QCL epitaxial layers to an InGaAs passive waveguide has been shown by monolithic growth on the native InP substrate [16].

In this paper, we review our previous integration approaches of ICLs and QCLs on silicon. Section II discusses various aspects of the waveguide platform, including differences from the materials employed at shorter wavelengths and beam combining. This is followed in Section III by a review of the first ICLs integrated on SOI waveguides. Section IV reviews our recent realization of beam combining of individual QCLs, while Section V reports new results of QCLs integrated on Ge-on-Si waveguides.

## II. WAVEGUIDE PLATFORM

As wavelength increases beyond the telecom band, absorption of the BOX layer increases rapidly as a function of wavelength beyond  $4 \mu\text{m}$ . Low loss waveguides and photodetectors integrated with spectrometers have been realized on a  $400 \text{ nm}$  silicon waveguide layer at  $3.8 \mu\text{m}$  [17], [18]. The wavelength of operation has been increased to  $7.67 \mu\text{m}$  by removing the BOX layer below the waveguide and making them free standing [19]. While the free-standing waveguide approach can provide high performing passive devices, it is a poor choice for laser integration since the heat dissipation becomes very ineffective. To extend the suitability of the silicon-based waveguide platform to wavelengths beyond  $4 \mu\text{m}$ , either the thickness of the waveguide core must be increased (to minimize absorption in the cladding

of an SOI waveguide) or alternate materials must be chosen for greater transparency.

### A. SOI Waveguides

To make the SOI waveguides compatible beyond  $4 \mu\text{m}$ , we increased the waveguide core thickness to  $1500 \text{ nm}$  to reduce overlap of the fundamental mode with the highly absorptive  $2 \mu\text{m}$  thick BOX layer. Additional sources of propagation loss include the scattering loss from the sidewalls, free carrier absorption loss in the waveguide layer, and absorption losses originating in the deposited top cladding. A high resistivity ( $> 100 \Omega/\text{cm}^2$ ) silicon device layer was used to lower the free carrier absorption loss. A pulsed plasma based etching chemistry was developed in a deep reactive ion etching (DRIE) tool to minimize the sidewall scattering loss. To calculate the waveguide propagation loss, we fabricated SOI waveguides spirals with  $2 \mu\text{m}$  width and 15 different lengths ( $8 \text{ mm}$  to  $11 \text{ cm}$ ). Details of the measurement system are presented in [20]. Fig. 1(a) shows a SEM image of the waveguide, while Fig. 1(b) shows the simulated profile of the  $\text{TM}_{00}$  mode in the air clad and  $1 \mu\text{m}$  thick SiN clad waveguide. Two different types of SiN films ( $1 \mu\text{m}$  PECVD low stress and  $1 \mu\text{m}$  sputtered low stress) were deposited on separate chips. Fig. 1(c) shows the calculated propagation losses for all three waveguides. The propagation loss for the air-clad waveguides increases sharply beyond  $4.7 \mu\text{m}$ , confirming that the loss arises in the BOX layer. The loss of the top cladding is evaluated in order to identify the source of loss in heterogeneously-integrated lasers that use such a film for electrical isolation, since the silicon waveguides are typically left covered with the deposited film. The loss is found to be high in both films. For the PECVD film, the loss can be attributed to the silicon-hydrogen absorption band present near  $4.6 \mu\text{m}$ , while the higher loss in the sputter films at shorter wavelengths could arise from roughness in the deposited film.

### B. Ge-on-Si Waveguides

Ge-on-Si is an alternate waveguide platform which can cover a broad wavelength range ( $2\text{--}14 \mu\text{m}$ ) [21]–[23]. Both silicon and germanium are currently used in CMOS foundries. There have been reports of low loss Ge-on-Si waveguides and devices at wavelengths as long as  $11 \mu\text{m}$  [24]. Since the biggest challenge in this waveguide platform is loss arising from the high defect density at the silicon-germanium interface [25], the overlap of the mode with this interface has been reduced by increasing the Ge core thickness to  $2 \mu\text{m}$ . In our previous work, we demonstrated low-loss waveguides in fully-etched and partially-etched ( $1 \mu\text{m}$  etch depth) geometries. For partially-etched waveguides, the measured propagation loss was roughly  $1 \text{ dB/cm}$  across the  $4.5\text{--}5 \mu\text{m}$  wavelength range. Mach-Zehnder interferometers (MZIs) in  $1 \times 1$  and  $2 \times 2$  configurations, with low insertion loss and high extinction ratio [26], were also fabricated. These MZIs were designed using multi-mode interferometers (MMIs), and the difference in length of the delay lines was adjusted so as to obtain an FSR of  $25 \text{ nm}$ .

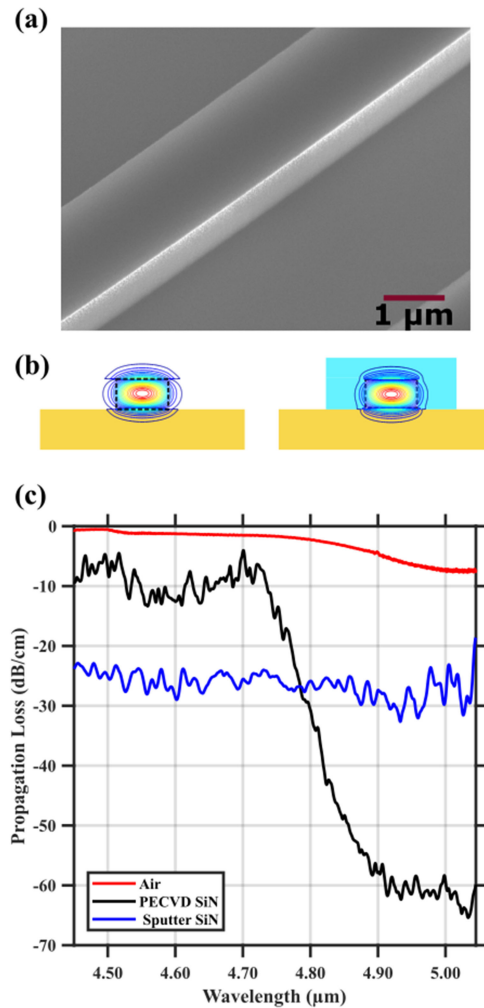


Fig. 1. (a) SEM image of a SOI waveguide etched using a deep reactive ion etching (DRIE) technique. A pulsed plasma technique is used to obtain vertical and smooth side walls. (b) Simulated mode profiles of the fundamental TM mode in air clad and SiN clad waveguides. The simulated confinement of the  $TM_{00}$  mode in the SiN layer is  $\sim 8.7\%$ . (c) Measured propagation loss of an air clad waveguides, a PECVD SiN clad waveguide and sputtered SiN clad waveguides.

### C. Beam Combiners

Beam combining different light sources in a single waveguide is an attractive solution for power scaling of integrated QCLs. Beam combiners in the form of arrayed waveguide gratings (AWGs) have been demonstrated on both SOI and Ge-on-Si waveguide platforms. An A WG allows beam combining of several channels with minimal power penalty, and the number of channels can be scaled if the design is robust. Furthermore, an A WG works as a spectrometer when operated in the reverse direction that separates a single input beam into spectral constituents. In that mode it is suitable for on-chip sensing applications.

For both of these purposes, the key challenge in designing the A WG is to maintain low insertion loss as well as low crosstalk between the channels. Crosstalk can occur in an A WG due to sidewall roughness or undesired coupling into higher-order modes, while insertion loss can result from inefficient light

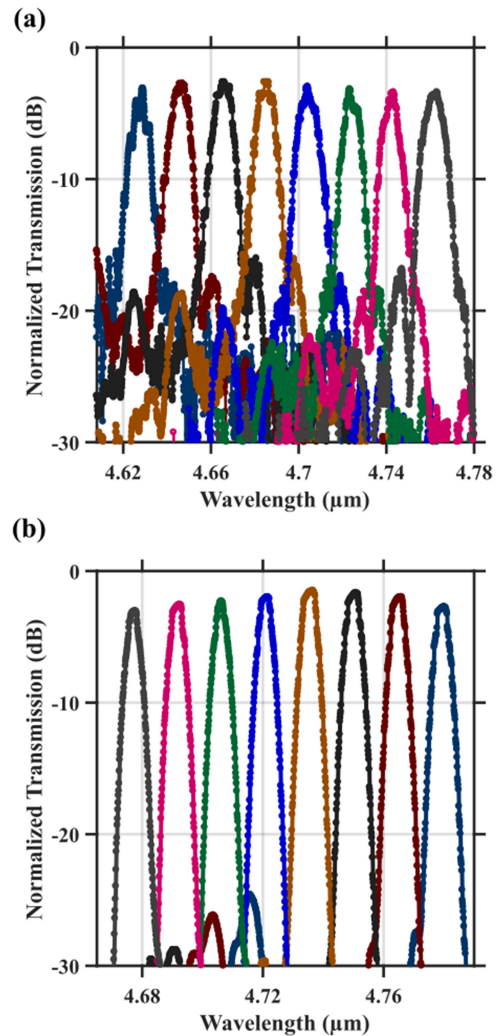


Fig. 2. Normalized spectra of 8 channel AWGs fabricated on (a) fully etched air clad SOI waveguide and (b) partially etched Ge-on-Si waveguides.

collection in the array waveguides. Both issues can be resolved by optimizing the A WG design.

In the SOI waveguide platform, the eight-channel A WG was designed with a channel spacing of 20 nm and array waveguide width of 1.5 μm. The measured sidemode suppression and insertion loss were  $-14$  dB and  $-2.6$  dB, respectively. The reason for such high crosstalk as compared to other reported A WGs designed with same methodology (described in [27]) can be attributed to phase errors arising from the narrow waveguide width. For the Ge-on-Si platform, A WGs were designed in both fully-etched and partially-etched geometries with 15 nm channel spacing and 4 μm waveguide width. The measured sidemode suppression and insertion loss were  $-28$  dB and  $-3.24$  dB for the fully-etched A WG, and  $-25$  dB and  $-1.54$  dB for the partially-etched A WG. Clearly sidewall roughness effects were minimal for the wider waveguides.

The A WGs presented above can be used for on-chip tunable diode laser spectroscopy (TDLAS) if the pass band of the A WG aligns with the absorption peak of the analyte. In case a larger



measurement bandwidth is required, then either the design of the AWG itself can be modified (by increasing the number of channels or by making the AWG cyclic) or an adiabatic beam combiner can be used [28].

### III. INTERBAND CASCADE LASERS ON SILICON

Interband cascade lasers emit via interband optical transitions between electron states in the conduction band and hole states in the valence band of GaSb-based quantum wells [11]. Band structure engineering in the ICL design provides electron-hole creation at a semimetallic interface in each stage, tuning of the emission wavelength with quantum well thickness, high gain from the type-II “W” band alignment [29], and efficient cascaded current injection into successive stages, while maintaining a much longer upper-state lifetime than in a QCL because the transitions are interband. Moreover, Auger recombination is suppressed by the type II band structure [30] and “carrier rebalancing” [31] associated with heavy doping of the electron injectors. Consequently, mid-IR light generation in an ICL is possible at much lower power budget than in a QCL [30].

We integrated ICLs with central operational wavelength of  $3.65\ \mu\text{m}$  on SOI waveguides to realize FP lasers [32]. Lasers with mesa widths of  $11\ \mu\text{m}$ ,  $8\ \mu\text{m}$  and  $6\ \mu\text{m}$  were fabricated. The integration of GaSb-based light sources on silicon waveguides has proved challenging in past, as the processing of GaSb compounds differs considerably from InP-based compounds and several modifications in the fabrication scheme are needed to insure high yield of devices. In this case the ICL layering was designed to provide good laser performance, while allowing a suitable tolerance in the processing. The resulting design was therefore not fully optimized for the efficient transfer of light between the laser mesa and the passive silicon waveguides.

Fig. 3(a) shows the LIV characteristics of an integrated ICL with III-V mesa width  $11\ \mu\text{m}$  at different temperatures, after removal of the adiabatic taper transitions to the SOI waveguide. The lasers were characterized for 175–250 ns pulses at a frequency of 1 KHz. The threshold current density for this laser at  $20^\circ\text{C}$  was  $1.1\ \text{kA}/\text{cm}^2$ , while the corresponding threshold current density for a laser with  $11\ \mu\text{m}$ -wide III-V mesa was  $1.45\ \text{kA}/\text{cm}^2$ . The maximum peak output power measured for an ICL-on-Si at room temperature was 6.6 mW, which is much lower than is typical for an ICL fabricated on the native GaSb substrate. The output of the integrated laser is limited mostly by significant sidewall leakage, which is evidenced by both a soft electrical turn-on in the I-V characteristic and a near-independence of the threshold current on III-V mesa width. Sidewall leakage is known to be less problematic in ICLs when a methane-based RIE (unavailable to this processing) is employed rather than the  $\text{BCl}_3$ -based etch used for the present devices [33].

The spectral characteristics of the FP lasers show lasing near  $3.6\ \mu\text{m}$ . The spectra before and after removing the III-V taper from one end show evidence of a coupled cavity formed by reflections between the remaining taper tips and cleaved silicon facets.

As seen in Fig. 3(b), the far field profile of light emitted from the hybrid III-V/SOI facet along the horizontal direction for a

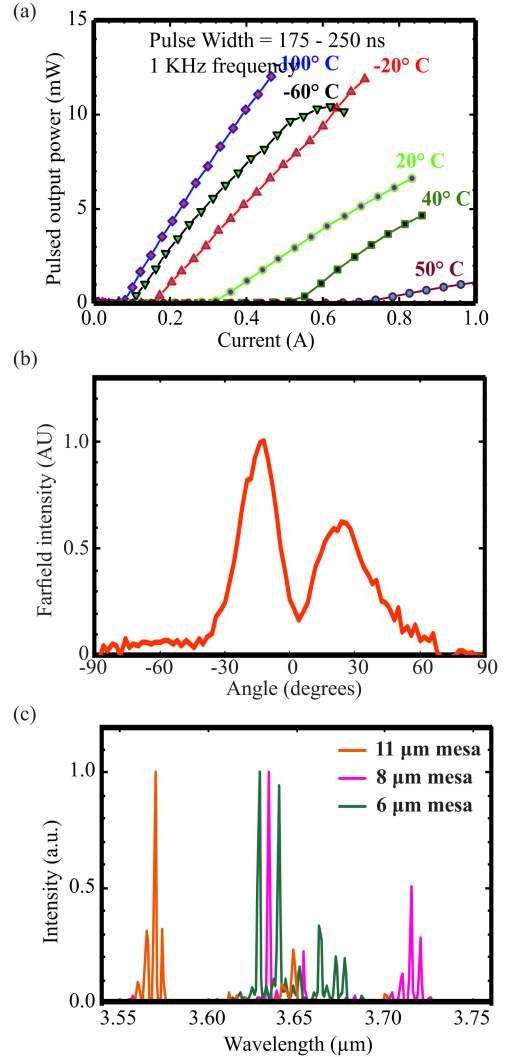


Fig. 3. (a) Pulsed LIV characteristics at various temperatures of an ICL integrated on SOI with  $11\ \mu\text{m}$  III-V mesa width, after one taper was removed, (b) horizontal far field profile of light emitted from the hybrid facet and (c) spectra from three different lasers collected after removing one taper.

device with  $8\ \mu\text{m}$  III-V mesa width indicates lasing in both the fundamental and higher order modes. The central minimum near zero angle was even more pronounced for a device with  $6\ \mu\text{m}$  III-V mesa width, but less so for a device with  $11\ \mu\text{m}$  mesa width. This indicates that the observation of lasing primarily in the second-order mode resulted mostly from the concentration of current flow (and hence gain) near the mesa sidewalls, rather than occurring because the mesa was too wide to assure preference for the fundamental mode. Clearly the observed mode profile affected the performance of the adiabatic tapers, which were designed for transfer of the  $\text{TE}_{00}$  mode to the underlying single mode silicon waveguide.

Fig. 3(c) shows the measured spectra from a hybrid facet of devices with various mesa widths. All of the spectra exhibit a mode selection arising from the second taper which has not been polished.

In spite of the challenges presented by the complicated fabrication scheme and excessive sidewall leakage of the integrated

ICLs, the devices operated in pulsed mode to 50 °C. The extracted  $T_0$  and  $T_1$  parameters of 43 K and 71 K, respectively, match well with those for ICLs processed on the native substrate. The tuning of the thermal gain peak tuning was measured to be 2.4 nm/°C. These results provide promising indications that with improvements in the design to increase the modal overlap with the passive silicon waveguide, and improvements in the fabrication to reduce the sidewall leakage, integrated ICLs will exhibit much better performance that is suitable for power scaling and on-chip spectroscopy.

#### IV. BEAM COMBINING OF DFB QCLS

QCLs use intersubband transitions within the conduction band to produce photons. In tunable diode laser spectroscopy (TDLAS), the wavelength emitted by a single-frequency laser source is swept across the absorption spectrum of a given molecular species. While a typical QCL gain spectrum is broad enough to span the absorption features of several different molecules, a given DFB QCL with limited temperature and current tuning range can generally cover only a single species. To broaden the bandwidth, one needs either a widely-tunable light source or beam combining. Beam combining with an AWG can provide much broader spectral coverage, since multiple lasers on a chip can employ different grating pitches that produce emission spanning the full gain bandwidth of the QCL. Furthermore, AWGs can combine the outputs of multiple epitaxial III-V gain chips emitting in different wavelength bands. AWGs can also provide power scaling via spectral beam combining, by coupling multiple single-frequency input beams into a single output waveguide.

We recently demonstrated AWG beam combining of two different types of QCLs to produce multi-spectral output from a single waveguide [34]. One group of lasers were designed in a DFB configuration. The DFB grating was realized by etching 23 nm into the underlying 1500 nm thick silicon waveguide, with a quarter wave shift introduced in the middle of the cavity to promote the selection of a single mode. The second group of QCLs were designed with a 1-mm-long DBR grating on the back end and a 0.5-mm-long grating on the front end of each laser cavity. While the DBR lasers emitted more than a single wavelength, their output was more likely to be aligned with the AWG passband. Both groups had 4-mm-long gain sections. The AWG passbands did not affect the emission wavelengths, since feedback was provided solely by gratings outside the AWG.

When tested individually, the integrated QCLs operated up to 60 °C under pulsed operation, and provided 2.5 mW of power from the output facet of the passive silicon waveguide. This increased to 83 mW when the taper was polished off of one end to reveal a hybrid waveguide facet.

Due to limited yield, only three of eight DFB lasers and two of eight DBR lasers integrated with AWGs provided significant light. Fig. 4 shows LIV characteristics and spectra measured from the front facet of the AWG when the lasers are operated with 500 ns wide pulses. Clearly, the output power scales when multiple devices are operated simultaneously and input to the

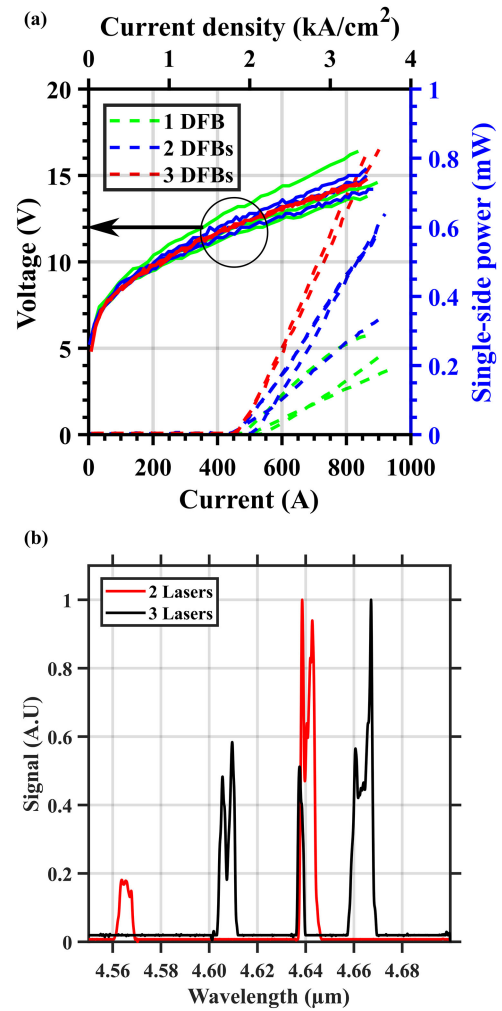


Fig. 4. (a) LIV characteristics of beam-combined DFB QCLs. Power scaling is evident, as the brightness increases with increasing number of operational lasers. (b) Output spectra from the AWG while driving three lasers simultaneously and two lasers simultaneously.

AWG. The data also confirm that the performance is unaffected by thermal crosstalk between the lasers, since there is no clear relationship between the total output power and proximity of the lasers to each other. Most probably, the output power decreases because a single current source drives all the lasers at once, and each laser has a slightly different resistance that results in a different drawn current. The multiple peaks in the emission spectra come from the unwanted reflections from the QCL to passive waveguide taper.

#### V. QCLS ON Ge-ON-Si WAVEGUIDE PLATFORM

The hybridization of QCLs with Ge-on-Si waveguides provides a way to realize integrated lasers in the long wave infrared, where an SOI waveguide would be excessively lossy due to absorption in the BOX layer. Previous heterogeneously-integrated lasers have used adiabatic tapers to transfer light between the III-V mesa and the passive silicon waveguide. The adiabatic taper works on the principle that if two waveguides of different widths are brought close to each other and their width is altered

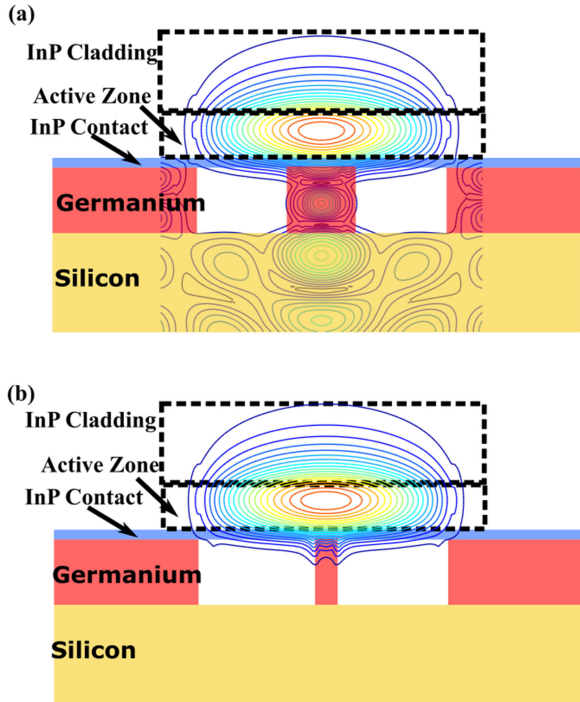


Fig. 5. Contour plot showing the fundamental TM mode confined in the QCL mesa integrated on a Ge-on-Si waveguide for (a)  $2\ \mu\text{m}$  wide Ge waveguide and (b) a  $600\ \text{nm}$  wide Ge waveguide.

simultaneously in inverse direction, light can be coupled from one waveguide to another without any reflections. This principle works well for InP based lasers operating in telecom wavelength band integrated on SOI waveguides [35]. However, it is more challenging to couple the output from a QCL into Ge-on-Si waveguides due to the high refractive index of the Ge and the lack of a low index cladding. To avoid substrate leakage of the lasing mode, the effective index should exceed the refractive index of silicon. For example, for a  $2\ \mu\text{m}$  tall and  $2\ \mu\text{m}$  wide Ge waveguide, Fig. 5(a) shows that the mode with the highest confinement within the III-V gain portion of the active hybrid waveguide mesa leaks into the silicon substrate, which will cause high propagation loss. In contrast, a  $2\text{-}\mu\text{m}$ -thick passive Ge waveguide with air clad and  $600\text{-nm}$  width [Fig. 5(b)] should support a single mode without significant leakage at  $4.6\ \mu\text{m}$  wavelength.

The III-V bond yield is also particularly important when QCLs are integrated on Ge-on-Si waveguides. Because germanium etches in many of the wet and dry etch chemistries used to fabricate QCLs [36], [37], passive Ge waveguides can be damaged during the laser fabrication in regions where the III-V bond fails.

In our first set of integrated QCLs on Ge-on-Si waveguides, light is not coupled from the III-V/GOS active region to the passive Ge-on-Si waveguides. The width of the Ge waveguide was kept below  $600\ \text{nm}$  to avoid leakage to the silicon substrate. The lasers themselves are designed with tapers on both ends, to allow a determination of whether any coupling occurs via other mechanisms such as evanescent coupling [38] or mode beating.

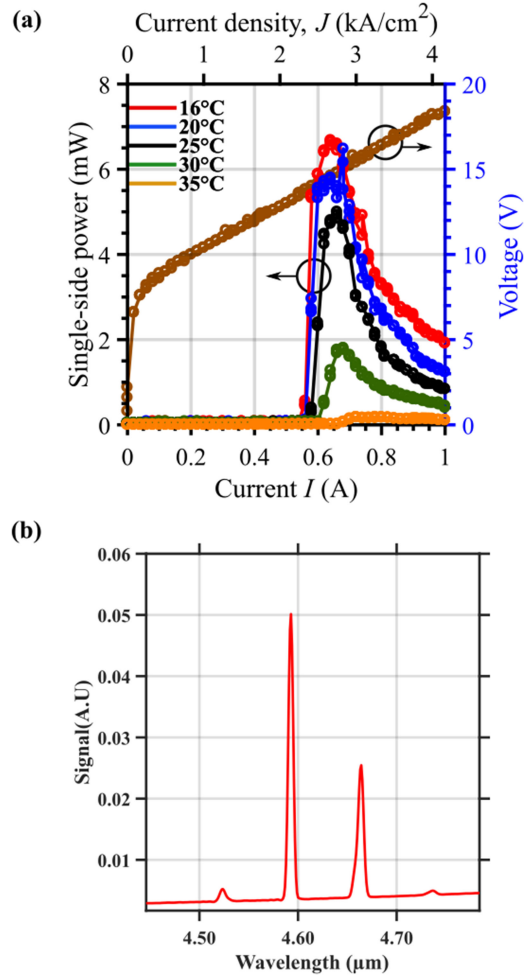


Fig. 6. (a) LIV characteristic of QCLs integrated on Ge-on-Si waveguides. The laser mesa is  $6\ \mu\text{m}$  and the length is  $4\ \text{mm}$ . (b) Measured spectrum of the laser.

The fabrication of these integrated QCLs is done quite similar to standard heterogeneously integrated lasers. First the germanium waveguide is patterned together with the outgassing vertical channels following which bonding of QCL epitaxial layer (grown at the University of Wisconsin) is carried out. The InP substrate is then thinned down to  $\sim 150\ \mu\text{m}$  thickness mechanically and then etched in a HCl:DI (1:3) solution. The p-mesa is then defined in methane/hydrogen/argon based dry etch chemistry using  $\text{SiO}_2$  as hard mask. For active region etching, the desired photoresist pattern is defined and then the sample etched for 20 seconds in a  $\text{H}_3\text{PO}_4:\text{H}_2\text{O}_2:\text{H}_2\text{O}$  solution followed by a 5-minute DI water rinse. The photoresist is then removed and the process is repeated seven times. A  $1\ \mu\text{m}$  thick low stress PECVD  $\text{SiN}$  cladding is deposited and vias are opened for metal deposition. The samples are then diced and polished.

When both the tapers were present, the measurements of these lasers showed only LED-like output. This indicated that the taper structures cause too much loss. The amount of light emitted from the germanium waveguide was insufficient for any spectral measurements using the FTIR. To evaluate whether the lasers survived processing, the tapers were polished and the

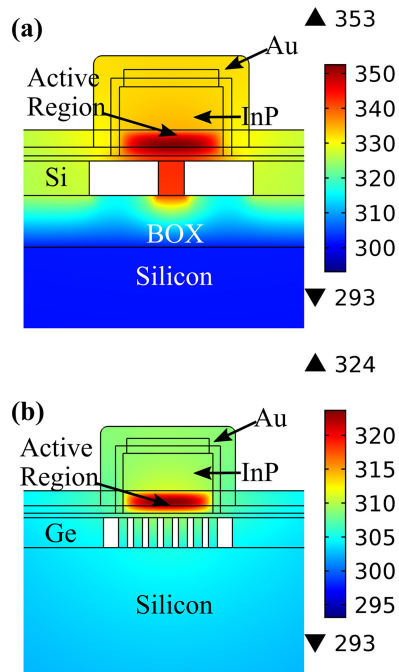


Fig. 7. Comsol simulations of the heat generated in QCLs integrated on: (a) an SOI waveguide and (b) a Ge-on-Si waveguide. The QCLs with 2 mm length are assumed to be driven by 500 mA of current and 17 V. The temperature reduction in the device with Ge rails and no BOX layer is clear.

integrated lasers were measured using a pulsed current source with 500 ns wide pulses at a duty cycle of 5%. Fig. 6(a) shows LIV characteristics of the integrated QCLs with 4-mm gain section at different temperatures and Fig. 6(b) shows the spectra measured using a Bruker FTIR system.

The LIV characteristics show that the threshold current of the integrated QCLs is much higher than those integrated on SOI or SONOI waveguides. A possible reason behind this could be the fact that the laser mesa is suspended mostly in air and it is extremely difficult to obtain a nicely polished facet. Several defects were observed in a microscope image of the polished III-V/germanium hybrid facet. The spectrum shows multiple peaks, which are not evenly spaced. This indicates wavelength selective feedback from the defects present on polished facets.

One way of improving the thermal performance of these devices is to provide an effective heat sink to the QCL mesa that does not introduce too much optical loss. For example, a heat sink could be provided by including multiple germanium rails below the QCL mesa. Fig. 7 illustrates a thermal analysis of QCLs integrated on both SOI and Ge-on-Si waveguides with multiple rails, using commercially available Comsol software. For a current of 0.5 A injected in the active region, both lasers heat up considerably. However, the heat generated in the laser integrated on a SOI waveguide, with a silicon waveguide of width 1.5  $\mu\text{m}$ , spreads poorly due to high thermal impedance of the BOX layer. For the same amount of injected current, the maximum temperature of the laser integrated on top of germanium rails is 25  $^{\circ}\text{C}$  lower. The fundamental mode of this waveguide does not leak to the substrate, since the width of

each individual germanium rail is 600 nm. This indicates that with proper waveguide engineering and thermal management, integrated QCLs can be realized on Ge-on-Si waveguides, and the wavelength of operation can be pushed in the long wave infrared.

## VI. CONCLUSION

In this review, we have discussed various aspects of integrated mid-infrared lasers, detailing the passive waveguide platforms, integration of ICLs and QCLs on SOI waveguides, beam combining of multiple lasers using AWGs and the first demonstration of integrated QCLs on Ge-on-Si waveguides. Choosing an appropriate waveguide platform with low propagation loss is critical for high performance mid-infrared photonic integrated circuits. Low-stress PECVD SiN claddings appear to have increased absorption at wavelengths past  $\sim 4.7 \mu\text{m}$  compared to sputtered SiN claddings, but further development is needed to construct silicon waveguides with an upper SiN cladding with propagation loss levels appropriate for low-loss integrated devices.

It should be possible to demonstrate high power, continuous wave, room temperature ICLs by optimizing the epitaxial design for increased overlap with the passive silicon waveguide, and by reducing the sidewall leakage after improving the fabrication process with a different dry etch.

The beam-combined lasers can also be designed in a different configuration by including the AWG in the laser cavity to avoid any extra loss coming from misalignment of the individual lasers with the AWG passband. This could be an attractive way to increase the optical throughput of the beam combined lasers.

We have carried out a proof-of-principle demonstration of integrated QCLs on Ge-on-Si waveguides. Further strategies, such as evanescent coupling, are currently being explored to efficiently couple light from the QCL mesa to a passive germanium waveguide.

These developments prove that the integration of mid infrared light engines with silicon waveguides will enable the realization of compact light sources with novel functionalities. The U.S. Government is authorized to reproduce and distribute reprints for Governmental purposes notwithstanding any copyright notation thereon. The views and conclusions contained herein are those of the authors and should not be interpreted as necessarily representing the official policies or endorsements, either expressed or implied, of Air Force Research Laboratory or the U.S. Government.

## ACKNOWLEDGMENT

The authors would like to thank Dr. Thomas Nelson Jr. from the Air Force Research Laboratory for useful discussions.

## REFERENCES

- [1] J. E. Bowers, "A path to 300 mm hybrid silicon photonic integrated circuits," in *Proc. Opt. Fiber Commun. Conf. Expo.*, San Francisco, CA, USA, Mar. 2014, pp. 11–13.



- [2] S. Romero-García *et al.*, “Edge couplers with relaxed alignment tolerance for pick-and-place hybrid integration of III–V lasers with SOI waveguides,” *IEEE J. Sel. Topics Quantum Electron.*, vol. 20, no. 4, Jul./Aug. 2014, Art. no. 8200611.
- [3] G. Roelkens *et al.*, “III–V/silicon photonics for on-chip and inter-chip optical interconnects,” *Laser Photon. Rev.*, vol. 4, no. 6, pp. 759–779, 2010.
- [4] D. Huang *et al.*, “High-power sub-kHz linewidth lasers fully integrated on silicon,” *Optica*, vol. 6, no. 6, pp. 745–752, 2019.
- [5] S. Dhoore *et al.*, “Electronically tunable distributed feedback (DFB) laser on silicon,” *Laser Photon. Rev.*, vol. 13, no. 3, 2019, Art. no. 1800287.
- [6] R. Jones *et al.*, “Heterogeneously integrated InP/silicon photonics: Fabricating fully functional transceivers,” *IEEE Nanotechnol. Mag.*, vol. 13, no. 2, pp. 17–26, 2019.
- [7] C. Zhang and J. E. Bowers, “Silicon photonic terabit/s network-on-chip for datacenter interconnection,” *Opt. Fiber Technol.*, vol. 44, pp. 2–12, 2017.
- [8] R. Wang *et al.*, “Broad wavelength coverage 2.3  $\mu\text{m}$  III–V-on-silicon DFB laser array,” *Optica*, vol. 4, no. 8, pp. 972–975, 2017.
- [9] R. Wang *et al.*, “Compact GaSb/silicon-on-insulator 2.0x  $\mu\text{m}$  widely tunable external cavity lasers,” *Opt. Express*, vol. 24, no. 25, 2016, Art. no. 28977.
- [10] A. Spott *et al.*, “Heterogeneously integrated 2.0  $\mu\text{m}$  CW hybrid silicon lasers at room temperature,” *Opt. Lett.*, vol. 40, no. 7, pp. 1480–1483, 2015.
- [11] I. Vurgaftman *et al.*, “Interband cascade lasers,” *J. Phys. D*, vol. 48, 2015, Art. no. 123001.
- [12] C. Gmachl *et al.*, “Recent progress in quantum cascade lasers and applications,” *Rep. Prog. Phys.*, vol. 64, pp. 1533–1601, 2001.
- [13] A. Spott *et al.*, “Quantum cascade lasers on silicon,” *Optica*, vol. 3, pp. 545–551, 2016.
- [14] A. Spott *et al.*, “Heterogeneously integrated distributed feedback quantum cascade lasers on silicon,” *Photonics*, vol. 3, p. 35, 2016.
- [15] H. Nguyen-Van *et al.*, “Quantum cascade lasers grown on silicon,” *Scientific Reports*, vol. 8, 2018, Art. no. 7206.
- [16] S. Jung *et al.*, “Homogeneous photonic integration of mid-infrared quantum cascade lasers with low-loss passive waveguides on an InP platform,” *Optica*, vol. 6, no. 8, pp. 1023–1030, 2019.
- [17] M. Muneeb *et al.*, “Demonstration of silicon-on-insulator mid-infrared spectrometers operating at 3.8  $\mu\text{m}$ ,” *Opt. Express*, vol. 21, pp. 11659–11669, 2013.
- [18] M. Muneeb *et al.*, “III–V-on-silicon integrated micro-spectrometer for the 3  $\mu\text{m}$  wavelength range,” *Opt. Express*, vol. 24, no. 9, pp. 9465–9472, 2016.
- [19] J. S. Penadés *et al.*, “Suspended silicon waveguides for long-wave infrared wavelengths,” *Opt. Lett.*, vol. 43, pp. 795–798, 2018.
- [20] A. Malik *et al.*, “High performance  $7 \times 8$  Ge-on-Si arrayed waveguide gratings for the midinfrared,” *IEEE J. Sel. Topics Quantum Electron.*, vol. 24, no. 6, Nov./Dec. 2018, Art. no. 8300108.
- [21] A. Malik *et al.*, “Germanium-on-silicon mid-infrared arrayed waveguide grating multiplexers,” *IEEE Photon. Technol. Lett.*, vol. 25, no. 18, pp. 1805–1808, Sep. 2013.
- [22] M. Nedeljkovic *et al.*, “Germanium-on-silicon waveguides operating at mid-infrared wavelengths up to 8.5  $\mu\text{m}$ ,” *Opt. Express*, vol. 25, no. 22, pp. 27431–27441, 2017.
- [23] R. Soref, “Mid-infrared photonics in silicon and germanium,” *Nature Photon.*, vol. 4, pp. 495–497, 2010.
- [24] K. Gallacher *et al.*, “Low loss Ge-on-Si waveguides operating in the 8–14  $\mu\text{m}$  atmospheric transmission window,” *Opt. Express*, vol. 26, no. 20, 2018, Art. no. 334988.
- [25] A. Malik *et al.*, “Silicon-based photonic integrated circuits for the mid-infrared,” *Procedia Eng.*, vol. 140, pp. 144–151, 2016.
- [26] A. Malik *et al.*, “Ge-on-Si wavelength division multiplexing components near 4.7  $\mu\text{m}$ ,” in *Proc. Conf. Lasers Electro-Optics*, 2018, Paper JW2A.39.
- [27] E. J. Stanton *et al.*, “Low-loss demonstration and refined characterization of silicon arrayed waveguide gratings in the near-infrared,” *Opt. Express*, vol. 25, no. 24, pp. 30651–30663, 2017.
- [28] E. Stanton *et al.*, “Multi-octave spectral beam combiner on ultra-broadband photonic integrated circuit platform,” *Opt. Express*, vol. 23, no. 9, pp. 11272–11283, 2015.
- [29] J. R. Meyer *et al.*, “Type-II quantum-well lasers for the mid-wavelength infrared,” *Appl. Phys. Lett.*, vol. 67, p. 757, 1995.
- [30] I. Vurgaftman *et al.*, “Interband cascade lasers with low threshold powers and high output powers,” *IEEE J. Sel. Topics Quantum Electron.*, vol. 19, no. 4, Jul.–Aug. 2013, Art. no. 1200120.
- [31] I. Vurgaftman *et al.*, “Rebalancing of internally generated carriers for mid-IR interband cascade lasers with very low power consumption,” *Nature Commun.*, vol. 2, p. 585, 2011.
- [32] A. Spott *et al.*, “Interband cascade laser on silicon,” *Optica*, vol. 5, no. 8, pp. 996–1005, 2018.
- [33] M. Kim *et al.*, “Interband cascade lasers with high CW power and brightness,” *Proc. SPIE*, vol. 9370, 2015, Art. no. 9370029.
- [34] E. J. Stanton *et al.*, “Multi-spectral quantum cascade lasers on silicon with integrated multiplexers,” *Photonics*, vol. 6, no. 1, p. 6, 2019.
- [35] M. L. Davenport *et al.*, “Heterogeneous silicon/III–V semiconductor optical amplifiers,” *IEEE J. Sel. Topics Quantum Electron.*, vol. 22, no. 6, Nov./Dec. 2016, Art. no. 3100111.
- [36] M. Wada *et al.*, “Cleaning and surface preparation for SiGe and Ge channel device,” *Solid State Phenomena*, vol. 187, pp. 19–22, 2012.
- [37] J. Kim *et al.*, “Germanium surface cleaning with hydrochloric acid,” *ECS Trans.*, vol. 3, no. 7, pp. 1191–1196, 2006.
- [38] S. Keyvaninia *et al.*, “Demonstration of a novel III–V-on-Si distributed feedback laser,” in *Proc. 2013 OFC/NFOEC*, Anaheim, CA, USA, 2013, pp. 1–3.



**Aditya Malik** received the bachelor’s degree from Delhi University, New Delhi, India, in physics, following which he joined the Indian Institute of Technology Delhi, New Delhi, India, for an M.Sc. program in physics.

He received the Ph.D. degree from the Photonics Research Group, Ghent University, Belgium, where he developed a novel CMOS compatible waveguide platform beyond the telecommunication wavelength range. After completing the Ph.D. degree, he worked on various topics, e.g., realizing integrated gas sensors, external cavity tunable lasers, and wavelength demultiplexers operating in mid-infrared. He is currently a Staff Scientist with the University of California, Santa Barbara, where his research focuses on heterogeneous integration of III–V materials on silicon-based waveguides in the datacom to mid-infrared wavelength range, high-speed low-energy consumption transceivers for datacom application, and passive silicon photonic devices. He was a DAAD Fellow with FU Berlin during the master’s studies. He has authored or coauthored more than 40 journals and conference papers, which have been cited more than 800 times.



**Alexander Spott** (S’10–GS’17) received the B.S. degree in physics from the University of Washington, Seattle, WA, USA, in 2011, the M.S. degree in electrical and computer engineering and the Ph.D. degree from the University of California, Santa Barbara, Santa Barbara, CA, USA, in 2015 and 2018.

His research interests include mid-infrared optoelectronics and silicon photonic integration. He has authored or coauthored more than 30 journals and conference papers, which have been cited more than 400 times. He was the recipient of a National Science

Foundation Graduate Research Fellowship in 2012.



**Eric J. Stanton** received the B.S. degree in electrical engineering from California Polytechnic State University San Luis Obispo, San Luis Obispo, CA, USA, in 2012, the M.S. degree in electrical and computer engineering and the Ph.D. degree from the University of California, Santa Barbara, Santa Barbara, CA, USA, in 2014 and 2018.

He is currently working with National Institute of Standards and Technology, Boulder, CO, USA.





Santa Barbara, Santa Barbara, in 2008.

**Jonathan D. Peters** has more than 13 years of process experience in the MEMS and semiconductor field. He was with the Applied Magnetics Corporation, Santa Barbara, as an Operator, Process Inspector, and Plate And Etch Technician for five years before moving to Solus Micro Technologies/NP Photonics, Westlake Village, as a Process Engineer for four years. He moved back to Santa Barbara to work with the Innovative Micro Technology as a Process Engineer and an R&D Engineer for four years before coming to work with the Bowers Group, University of California,



QW lasers. More recently, his research efforts have been focused on quantum cascade laser (QCL) design, fabrication, and testing, including research into high-power QCL phase-locked arrays.

**Jeremy Daniel Kirch** (M'12) was born in Madison, WI, USA, in 1983. He received the B.S. degree in both electrical engineering and physics in 2007 from the University of Wisconsin–Madison, Madison, where he is currently working toward the Ph.D. degree with the Department of Electrical and Computer Engineering as a Roger Bacon Fellowship recipient. His graduate studies primarily consisted of investigations into compressively strained metamorphic buffer layers grown by MOCVD on either InP or GaAs, including InAsP, InPSb, and InGaAs MBLs, for use with Type-I



semiconductor lasers using MOCVD crystal growth. He is the Co-Inventor of the resonant optical waveguide (ROW) antiguided array and has contributed to its development as a practical source of high coherent power, for which he received the TRW Group Level Chairman's Award. He developed a novel single-mode edge-emitting laser structure, the ARROW laser, as a source for coupling high powers into fibers. He is currently a Professor with the Department of Electrical and Computer Engineering, University of Wisconsin–Madison, where he is involved with the development of novel III/V compound semiconductor device structures, including vertical cavity surface emitters (VCSELs), active photonic lattice structures, dilute-nitride lasers, lasers employing metamorphic buffer layers, and quantum cascade lasers. Prof. Mawst has authored or coauthored more than 250 technical papers and holds 26 patents.

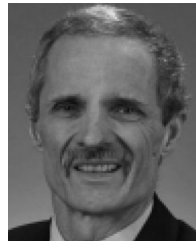
**Luke J. Mawst** (M'88–SM'93–F'11) was born in Chicago, IL, USA, in 1959. He received the B.S. degree in engineering physics and the M.S. and Ph.D. degrees in electrical engineering from the University of Illinois at Urbana-Champaign in 1982, 1984, and 1987, respectively. His dissertation research involved the development of index-guided semiconductor lasers and laser arrays grown by MOCVD.

He joined TRW, Inc., Redondo Beach, CA, in 1987, where he was a Senior Scientist in the research center, engaged in the design and development of



was a Senior Staff Scientist and a Technical Fellow. At TRW, he coined the concept of a resonantly (leaky-wave) coupled phase-locked laser array of antiguides (1988), which constituted the first photonic-crystal (PC) laser for single spatial-mode operation from wide-aperture ( $\geq 100 \mu\text{m}$ ) devices. As a result, in 1990, he led the team that “broke” the 1-W coherent-power barrier for diode lasers. Since 1993, he was the Philip Dunham Reed Professor of Electrical Engineering with the University of Wisconsin–Madison (UW–Madison), Madison. At UW–Madison, his initial research resulted in a record high CW power and wallplug efficiency from near-infrared diode lasers. Work on grating surface-emitting lasers in 2000 led to the concept of using a  $\pi$  phase shift in the grating center for single-lobe surface emission at no penalty in efficiency. Recent work has focused in two key research areas for mid-infrared, quantum cascade lasers: complete carrier-leakage suppression and PC-type devices for realizing single spatial-mode operation to watt-range CW powers. He has authored or coauthored more than 450 technical publications (H-index: 46) of which more than 350 were refereed, and holds 56 patents.

Prof. Botez is a member of Phi Beta Kappa and a Fellow of the Optical Society of America (OSA). In 1979, he received the RCA Outstanding Achievement Award for co-development of high-density optical recording using diode lasers. As part of the IEEE centennial (1984) events, he was chosen the Outstanding Young Engineer of the IEEE Photonics Society. In 1984, he co-initiated the IEEE Photonics Society Semiconductor Laser Workshop, which is now held annually. In 1995, he was awarded the “Doctor Honoris Causa” degree by the Polytechnical University of Bucharest, and in 2010, he was the recipient the OSA Nick Holonyak Jr. Award.



(H-index 58), 16 book chapters, 33 patents (seven licensed), and more than 160 invited conference presentations. He is a Fellow of the OSA, APS, IOP, and SPIE. He received the Presidential Rank Award, ONR's Captain Robert Dexter Conrad Award for Scientific Achievement in 2015, NRL's E. O. Hulbert Annual Science Award in 2012, and the IEEE Photonics Society Engineering Achievement Award in 2012.

**Jerry R. Meyer** (F'04) received the Ph.D. degree in physics from Brown University, Providence, RI, USA, in 1977. Since then, he has carried out basic and applied research at the Naval Research Laboratory, Washington, DC, USA, where he is the Navy Senior Scientist for Quantum Electronics (ST). His research has focused on semiconductor optoelectronic materials and devices such as new classes of semiconductor lasers and detectors for the infrared. He has coauthored more than 370 refereed journal articles, which have been cited more than 20 000 times



joining the UCSB. He has authored or coauthored eight book chapters, 700 journal papers, 900 conference papers, and is the recipient of 64 patents. He was the recipient of the IEEE Photonics Award, OSA Tyndal Award, OSA Holonyak Prize, IEEE LEOS William Streifer Award, and South Coast Business and Technology Entrepreneur of the Year Award. He and his coworkers were the recipient of the EE Times Annual Creativity in Electronics Award for most promising technology for the hybrid silicon laser in 2007. He is a member of the National Academy of Engineering and the National Academy of Inventors. He is a Fellow of the OSA and the American Physical Society.

**John E. Bowers** (F'94) received the M.S. and Ph.D. degrees from Stanford University, Stanford, CA, USA.

He holds the Fred Kavli Chair in nanotechnology, and is the Director of the Institute for Energy Efficiency and a Professor with the Departments of Materials and Electrical and Computer Engineering, University of California, Santa Barbara (UCSB), Santa Barbara, CA, USA. He is a Co-Founder of Aurion, Aeries Photonics, and Calient Networks. He was with the AT&T Bell Laboratories and Honeywell before